J. Mater. Environ. Sci. 7 (2) (2016) 390-396
ISSN : 2028-2508
CODEN: JMESCN

Effect of Na_2SiO_3 /NaOH mass ratio on the development of structure of an industrial waste-based geopolymer

N. Belmokhtar [*], L. Ben allal, S. Lamrani

Laboratoire des Matériaux et valorisation des ressources (LMVR)
Faculté des Sciences et Techniques de Tanger, University Abdelmalek Assaadi, BP 416, Tanger (Maroc)

**Corresponding Author. E-mail: belmokhtar2008@live.fr*

Abstract

The increase of industrial activity gives rise to an increase of quantity of solid waste that can have a negative impact on the environment and human life. Among these solid wastes, we can cite the industrial sludge. This study investigates the variation effect of $Na_2Si_2O_3$/ NaOH mass ratio on the development of structure of an industrial calcined sludge-based geopolymer. To reach this goal, a mechanical mixer was used to blend the calcined industrial sludge and the sodium silicate solution. The homogeneous paste obtained was poured into cylindrical molds and cured at room temperature under atmospheric pressure for 18 days, then at 50°C until compressive strength tests. The structural change of geopolymer based calcined industrial sludge was followed by FTIR spectroscopy, XRD and TEM analysis. The compressive strength of geopolymer specimens prepared from the calcined industrial sludge depends on the $Na_2Si_2O_3$/ NaOH ratio. The XRD analysis of geopolymer based calcined industrial sludge confirms that is an amorphous material. The micrographs obtained by MET of this material show the presence of a new solid phase in cluster form. The results obtained by FTIR spectroscopy indicate that the reaction between the calcined industrial sludge and the sodium silicate solution resulted in the formation of a new aluminosilicate phase rich with aluminum species.

Key-words: industrial sludge- geoploymer - alkali –activated material – FTIR study

Introduction

In recent year, there is an increase demand of development of new low-cost technologies that use the industrials wastes, especially the industrials wastes contaminated by the heavy metals [1,2]. The geopolymer cements and concretes can be a feasible way to manage a several industrial wastes, such as the industrial sludge contaminated by the heavy metals [3]. The studies carried out on geopolymer, confirm that this type of materials is a good heavy metal fixer, because during the geopolymerisation, the heavy metals are immobilized by chemical adsorption [4-6]. The presence of heavy metals affects the chemicals reactions and morphology structure, which causes the formation of different amorphous phases [3,7]. However, the heavy metals does not replace Al or Si of the tetrahedral building blocks of geopolymer [8,9]. The exact mechanism of geopolymerization is unknown due to the high speed of the reaction. However, several studies confirms that the geopolymerisation reaction is beginning by the dissolution of aluminosilicate material, and followed by the polycondensation of dissolved species in the three-dimensional network [1]. Several studies carried out on geopolymer cement have shown that the physicochemical and mechanical properties of these materials are strongly linking of the nature of the aluminosilicate source (mineralogical composition, degree of crystallinity), the nature of the alkali metal cations, the $Na_2Si_2O_3$/ NaOH ratio, H_2O/ NaOH ratio, the curing temperature and others [10–14]. The most alkali solution used to synthesize the geopolymer cement is the sodium silicate solution (mixture of water glass and sodium hydroxide solution) [15]. The several studies show that the

compressive strength of geopolymers cement increases with increasing Na_2SiO_3/NaOH ratio, due to the promotion of polymerization reaction [16]. The curing temperature has a significate effect on structural and mechanical properties of geopolymers (the increase of the curing temperature increase the compressive strength and decrease the setting time) [11],[17],[18]. The objective of this study is to evaluate the effect of variation of Na_2SiO_3 /NaOH mass ratio on the development of structure of calcined industrial sludge based geopolymer. In order to assess the feasibility of using this industrial waste as a geopolymer material.

2. Materials and methods.

2.1. Materials

The industrial sludge (B) used in this study was recuperated from a factory of ceramic products. Its chemical composition was determined by X-ray fluorescenceX and the result is shown in table 1. The molar ratio SiO_2/Al_2O_3 is 3.82. The industrial sludge was calcined at 800 ° C for 5 hours with a ramp as 5 °C/min in tubular furnace on open mode. When the calcination was completed, the sample was soaked in air, cooled at room temperature and placed in plastic bag. The BET surface area of calcined industrial sludge (MB800), determined by nitrogen adsorption on ASAP2010 instrument, is 2.37 m^2/g, and the medium laser particle size (d_{50}) is 7.12µm.

Table 1: chemical composition of industrial sludge (B) determined by X-ray fluorescence

Oxides	SiO_2	Al_2O_3	CaO	Na_2O	K_2O	ZrO_2	MgO	Fe_2O_3	ZnO	TiO_2
%	57,4	26,3	2,42	1,68	1,29	0,823	0,459	0,449	0,346	0,301

The sodium silicate solutions with different $Na_2Si_2O_3$/ NaOH mass ratios was prepared by adding the sodium hydroxide solution (12 M) to diluted water glass (Table 2). The sodium hydroxide solution was prepared by dissolution of NaOH grain (purity 97%) in distilled water. The solutions were cooled before adding the diluted water glass in various mass ratio. The sodium silicate solutions obtained are stored for 24 h before their use.

Table 2: chemical composition of water glass

	Si (mg/l)	**Na (mg/l)**
Compound	32.48	19.62

2.2. Geopolymer synthesis

The samples were prepared by mixing the calcined industrial sludge (MB800) and sodium hydroxide solutions for 10 minute, the mix proportions of pastes are shown in Table 3. After mixing, the fresh paste was casted into cylindrical molds (width=20mm and height = 40 mm) and they undergo twenty shocks for removing air bubbles trapped in the paste. Then the samples were cured at room temperature and normal pressure for 18 days then at 50°C until compressive strength tests.

Table 3: the mix proportions of pastes. $Na_2Si_2O_3$/ NaOH is the mass ratio of diluted water glass to sodium hydroxide solution; Si/Al is the molar ratio of Si to Al in the industrial sludge powder; S/L is the weight ratio of the industrial sludge to the sodium hydroxide solution.SiO_2/ Na_2O is the molar ratio of SiO_2 to Na_2O in diluted water glass

SAMPLES	$Na_2Si_2O_3$/ NaOH	Si/Al	S/L	SiO_2/ Na_2O
GEO0.8	0.8	1.92	1.2	3.19
GEO1	1	1.92	1.2	3.19
GEO1.2	1.2	1.92	1.2	3.19
GEO1.4	1.4	1.92	1.2	3.19

2.3. Characterization

The samples GEOn (n = 0.8, 1, 1.2 and 1.4) were examined by Fourier transform infrared spectroscopy (FTIR) by using KBr pellet technique, after 4 months of aging in the 4000-400 cm^{-1} range. The samples were prepared by mixing and grinding a small amount of geopolymer powder and potassium bromide (KBr) until a very fine powder. Then the mixture was pressed into a disk by using a mechanical press. The morphology of each sample was characterized by transmission electron microscopy (TEM) operating at 200 kV. XRD diagrams were obtained from powdered samples. The samples analyzed by XRD, MET were ground, and sieved at 80µm.

3. Results and discussion

3.1. XRD analysis.

The XRD patterrn of the calcined industrial sludge (MB800) and samples (GEO1 and GEO1.2) are presented in figure 1. The crystalline phases persistent in calcined industrial sludge are quartz and albite. The same crystalline phases are presented in geopolymers samples. This result signifies that the albite and quartz structure are not affected by the attack of the alkali activator. In the other hand, The absence of new crystalline phases proves the absence of zeolite structure[19]. The diffractograms of geopolymers samples show the presence of an halo between 23 and 34 (2theta), which in an indication of an amorphous phase formation. In the literature, this halo is attributed to a geopolymer material[20].

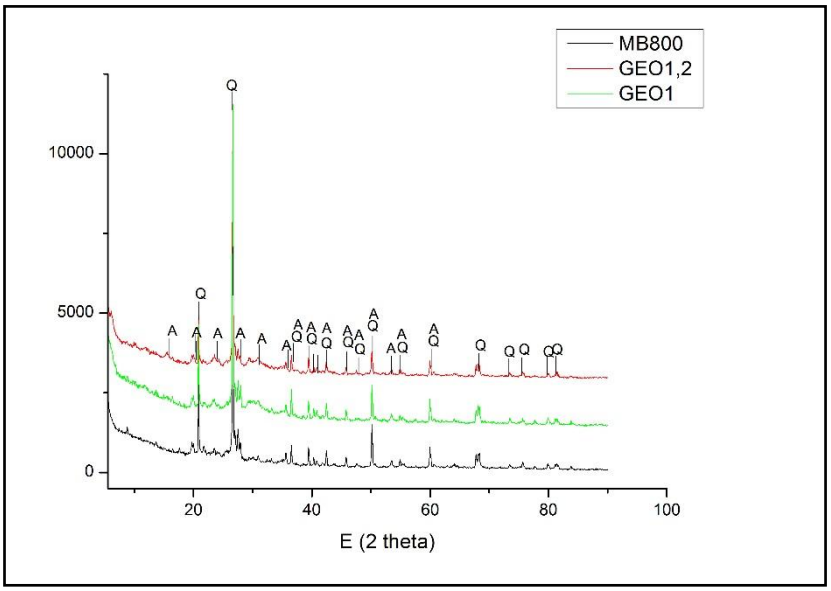

Figure 1: XRD pattern of calcined industrial sludge (MB800) and calcined industrial sludge based geopolymer (GEO1, GEO1.2). A: Albite; Q: Quartz.

3.2. TEM analysis.

TEM was used to examine the microstructural variations between the initial material (MB800) and MB800 based geopolymer (GEO0.8, GEO1, GEO1.2 and GEO1.4). The TEM micrographs for all samples are shown in figure 2. TEM analysis shown that the new formed material is a combination between the Nano-spherical precipitate[21] in cluster form and initial phases. All TEM micrographs of MB800 based geopolymer did not show any microcracking, this result shows that the thermal treatment at 50°C after 18 days of curing at ambient temperature leads to desiccate the geopolymer material without affecting the microstructure. The TEM micrographs reveal two types of reacted region. The first one is the fully reacted region (figure 2.d (1)) where the microstructure made up of spherical separated by nanoporosity in sponge-like microstructure. This kind of structure is shown in TEM micrographs of M-Metakaolin based geopolymer (M = Na or K). The second one is the partially reacted region (figure 2.b (2)) where the new formed microstructure is located on the original phases. The size of nanoparticules (approximately 10 nm [22]) and their forms (spherical form) confirm the

result obtained by XRD analysis, that the new formed structure is an amorphous phase. Comparing the extent of new formed phases shown in the micrograph of each sample, we can observe clearly the strong dependence of the extent of new formed phases with the mass ratio of activator solution compound, where the maximum extent was observed with $Na_2Si_2O_3/\ NaOH = 1.2$.

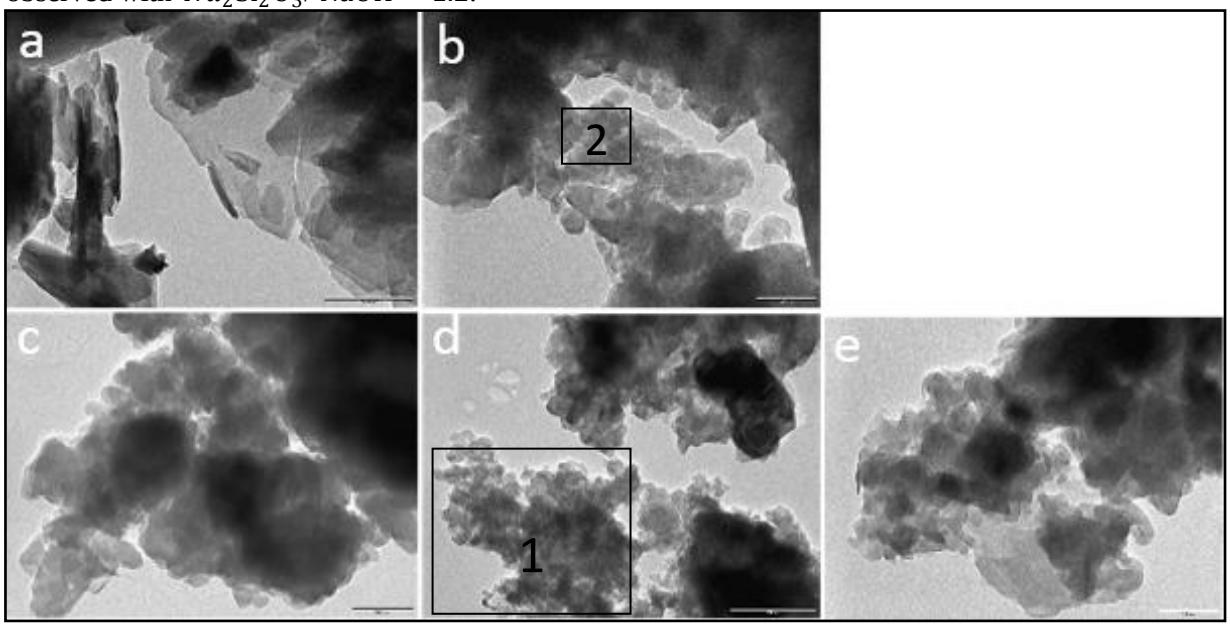

Figure 2: TEM micrographs of MB800 (a), GEO0.8 (b), GEO1 (c), GEO1.2 (d), and GEO1.4 (e).

3.3. FTIR analysis:

To assigning the peaks shown on the geopolymer spectra, we relied on the infrared studies carried out on Metakaolin based geopolymer [19], [23–25]. The change between the calcined and the raw industrial sludge appears clearly in their infrared spectra (figure 3). After calcination of the industrial sludge, the vibration bands of OH at 3696 cm^{-1} and 3619 cm^{-1} were disappeared. Which indicating that the kaolinite present in the industrial sludge was converted to Metakaolin.

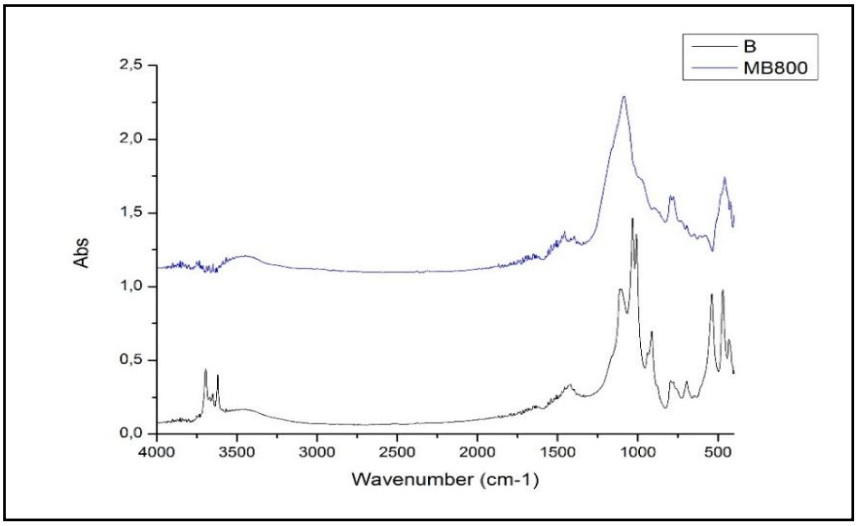

Figure 3: FTIR spectra of the raw industrial sludge (B) and calcined industrial sludge (MB 800)

The absorption band of kaolinite at 1104 cm^{-1} (Si-O-T in a crystal-network; T=Si or Al) has been moved to the lower frequency at about 1085 cm^{-1} (SiO_2 in an amorphous network). The disappearance of the absorption band of Al^{VI}-OH at 916 cm^{-1} and the intensity decrease of characteristic vibration of the Si-O at about 539 cm^{-1} together with its displacement to a higher frequency are due to the deformation of the tetrahedral and octahedral

sheets of the industrial sludge. This deformation brings about also the appearance of the band at 722cm^{-1} corresponding to the deformation vibration of Si-O-Si and Si-O-Al in the amorphous material (MB800). Thus the decrease of band intensity at 684 cm^{-1} (is attributed to the symmetric valence vibration of Si-O group).
The FTIR characterization of the geopolymer materials is given in figure 4. The broad absorption band between 3000- 3500 cm^{-1} and the band at 1652 cm^{-1} attributed to the vibration of H_2O absorbed at surface or entrapped in the new formed material cavities. The absorption bands at about 1415cm^{-1} indicates the existence of Na_2CO_3. The formation of these species is the result of the reaction of sodium hydroxide with the atmospheric CO_2 (efflorescence). The symmetric vibration band of Si-O-T at 1 085 cm^{-1} present in the FTIR spectrum of MB800 (figure 4) has been shifted to 979 cm^{-1}, 982 cm^{-1}, 989 cm^{-1} and 1007 cm^{-1} for GEO0.8, GEO1, GEO1.2 and GEO1.4 respectively. Which is explained by the formation of a new phase rich in Aluminum. The dissimilarity on the shift of the symmetric vibration band Si-O-T, could be attributed to the variation of $Na_2Si_2O_3$/ NaOH mass ratio. The shifted values exhibit that the increase of $Na_2Si_2O_3$/ NaOH mass ratio cause a decrease on the shift of Si-O-T band vibration. This phenomenon could be explained by the formation of poor aluminum phase when the $Na_2Si_2O_3$/ NaOH mass ratio grows, due to the increase of quantity of Si in the reaction medium. The absence of the intensity band at 865 cm^{-1} displays that the dissolution reaction of the initial calcined industrial sludge (MB800) was stopped. Therefore, the polycondensation reaction was stopped too.

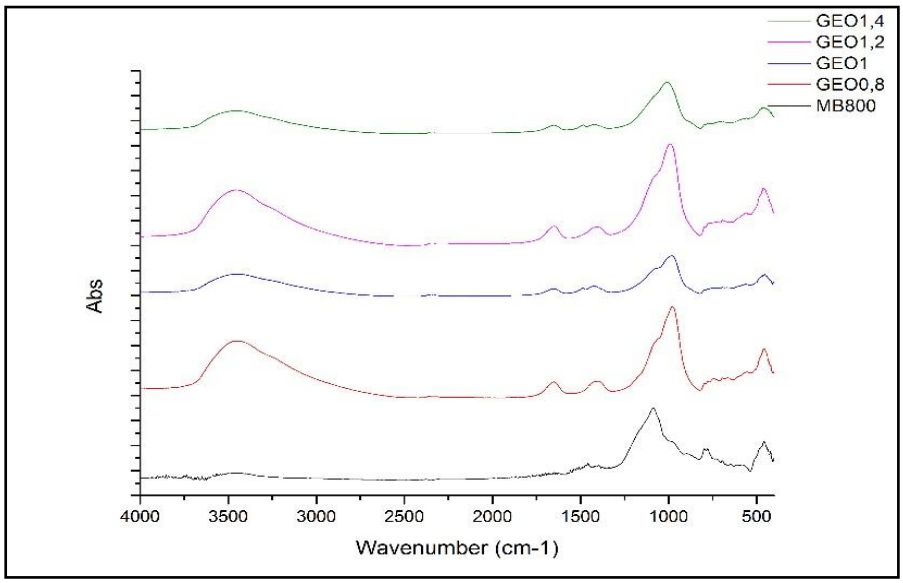

Figure 4: FTIR spectra ofMB800 and GEOn samples (n=0.8, 1, 1.2 and 1.4).

The infrared spectra shown in Figure 4 reveals that the major difference between the calcined industrial sludge and the geopolymer products is attributed to the displacement of the Si-O-T vibration bond (T=Si or Al) at low frequencies. This peak is the main peak in the infrared spectra of géopolymers synthesized from alumino-silicate powders. And as the intensity of this symmetric vibration depends on the amount of the Si-O-T bonds present in the new alumino-silicate phase formed, this peak could be used to show the variation effect of the $Na_2Si_2O_3$/ NaOH ratio on the formation of new Si-O-T. To obtain accurate results, we calculated the ratio of the peak intensity of new formed Si-O-T and that obtained at 459cm^{-1}. The intensity of the last peak depends on de concentration of Si-O and Al-O vibration bonds existing in the all phases (initial phases and new formed phases). The results are shown in Figure 5. We can note that the increasing of the ratio to 1.2 causes an increase in the number of Si-O-Al. However, the continuation of increasing $Na_2Si_2O_3$/ NaOH ratio leads to decreasing the number of Si-O-Al, which consequently decreases the production of the new phase characteristic of a geopolymer material. This result was already corroborated by the TEM analysis.

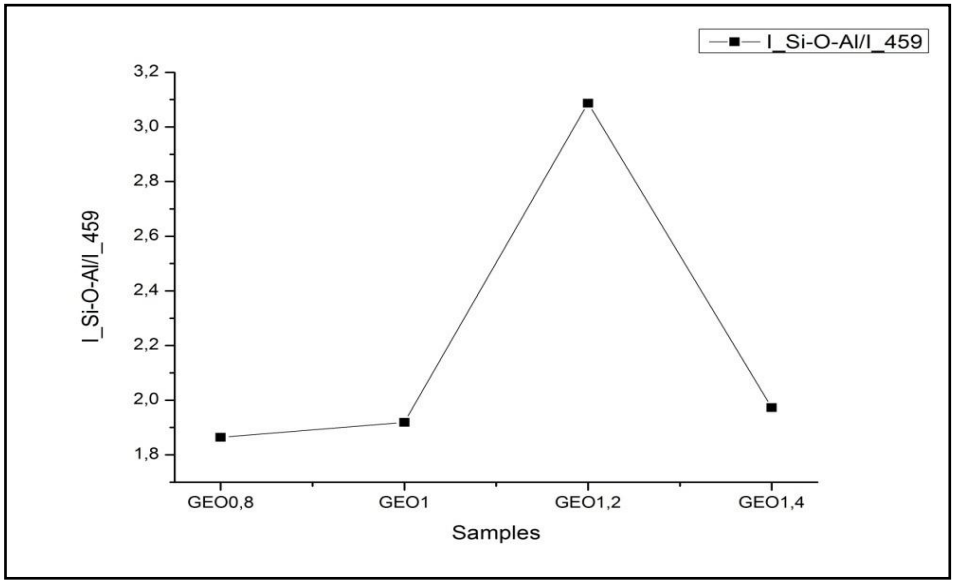

Figure 5: The relative intensity variation of Si-O-T vibration in the new formed structure as a function of Na_2SiO_3/NaOH mass ratio.

3.4. Compressive Strength testing

Figure 6 presents the compressive strength values of the four samples GEOn (n=0.8, 1, 1.2 and 1.4). With the Increasing of Na_2SiO_3/NaOH mass ratio from 0.8 to 1.2, we observe an increase in compression strength of the samples. This growth can be explained by the increase of the amount of the new aluminosilicate phase characteristic of geopolymer materials, which is confirmed also by TEM and FTIR analysis. However, the increase of Na_2SiO_3/NaOH mass ratio into 1.4 causes the decrease of compressive strength. This variation could also be attributed to the decrease of the amount of the new aluminosilicate phase characteristic of a geopolymer.

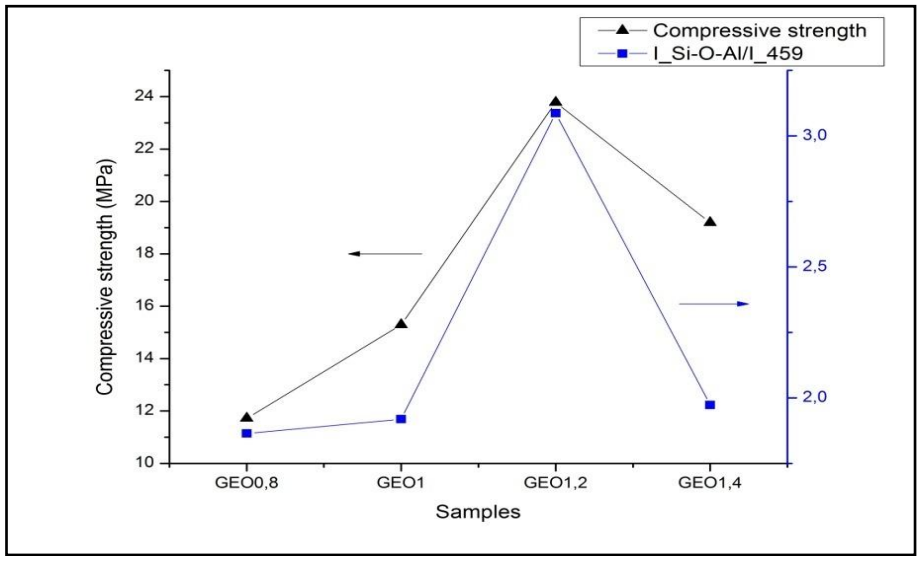

Figure 6: Compressive strength and relative intensity variations of GEOn (n=0.8, 1, 1.2 and 1.4)

Conclusion

In this study, the effect of Na2SiO3 /NaOH mass ratio on the development of structure of an industrial waste-based geopolymer was investigated by monitoring the structural changes they have undergone the samples. The results show that the calcination causes the deformation of the tetrahedral and octahedral sheets of the industrial sludge studied. The XRD analysis shows that the structure of geopolymers samples is amorphous. The new formed material is a combination between Spherical precipitates and initial phases. The activation of calcined

industrial sludge by diluted sodium silicate solution leads to the formation of a new phase rich in Aluminum, by polycondensation of dissolved species. The number of Silicate substituted by Aluminum depends on the $Na_2Si_2O_3$/ NaOH.The samples compressive Strength, follow the same variation of the relative intensity of the T-O vibration in the new phase formed.

References

1. Davidovits J., Geopolymer Chemistry and Applications, Geopolymer Institute, (2008).
2. El-Eswed B. I., Yousef R.I., Alshaaer M., Hamadnehd I.,Al-Gharablie S.I., Khalilid F., *International Journal of Mineral Processing*, 137 (2015) 34-42.
3. Provis J. L., van Deventer J. S. J., Geopolymers: Structures, Processing, Properties and Industrial Applications, Elsevier, (2009).
4. Ahmari S., Zhang L., *Construction and Building Materials*, 44 (2013) 743-750.
5. Xiaolu G., Huisheng S., Mingfeng X., *Journal of Wuhan University of Technology-Mater. Sci. Ed*. 28 (2013) 938-943.
6. Ge Y., Yuan Y., Wang K., He Y., Cui X., *Journal of Hazardous Materials*, 299 (2015) 711-718.
7. Cheng T. W., Lee M. L., Ko M. S., Ueng T. H., Yang S. F., *Applied Clay Science*, 56 (2012) 90-96.
8. Li Q., Sun Z., Tao D., Xu Y., Li P., Cui H., Zhai J., *Journal of Hazardous Materials*, 262 (2013) 325-331.
9. Steins P., Poulesquen A., Diat O., Frizon F., *Langmuir*., 28 (2012) 8502-8510.
10. Gao K., Lin K., Wang D., Hwang C., Shiu H., Chang Y., Cheng T., *Construction and Building Materials*, 53 (2014) 503-510.
11. Mo B., Zhu H., Cui X., He Y., Gong S., *Applied Clay Science*, 99 (2014) 144-148.
12. Lancellotti I., Catauro M., Ponzoni C., Bollino F., Leonelli C., *Journal of Solid State Chemistry*, 200 (2013) 341-348.
13. He J., Zhang J., Yu Y., Zhang G., *Construction and Building Materials*, 30 (2012) 80-91.
14. Pacheco-Torgal F., Castro-Gomes J., Jalali, S., *Cement and Concrete Research*, 37 (2007) 933-941.
15. Li C., Sun H., Li L., *Cement and Concrete Research*, 40 (2010) 1341-1349.
16. Mustafa Al Bakri A. M., Kamarudin H., Bnhussain M., Rafiza A. R., Zarina Y., *Materials Journal*, 109 (2012) 503-508.
17. Kong D. L. Y., Sanjayan J. G., Sagoe-Crentsil K., *Cement and Concrete Research*, 37 (2007) 1583-1589.
18. Khale D., Chaudhary R., *Journal of Materials Science*, 42 (2007) 729-746.
19. Rovnaník P., *Construction and Building Materials*, 24 (2010) 1176-1183.
20. Granizo M. L., Blanco-Varela M. T., Martínez-Ramírez S., *Journal of Materials Science*, 42 (2007) 2934-2943.
21. Autef A., Joussein E., Poulesquen A., Gasgnier G., Pronier S., Sobrados I., Sanz J., Rossignol S., *Journal of Colloid and Interface Science*, 408 (2013) 43-53.
22. Kriven W. M., Bell J. L., Gordon M., Advances in Ceramic Matrix Composites IX, John Wiley & Sons Inc., (2006).
23. Sun W., Li Z., *Journal of Wuhan University of Technology-Mater. Sci. Ed.* 23 (2008) 522-527.
24. Granizo M. L., Alonso S., Blanco-Varela M. T., Palomo A., *Journal of the American Ceramic Society*, 85 (2002) 225-231.
25. Autef A., Joussein E., Gasgnier G., Pronier S., Sobrados I., Sanz J., Rossignol S., *Powder Technology*, 250 (2013) 33-39.